ARTICLE NO. 78-1196R

Relation between Temporal and Spatial Stability in Three-Dimensional Flows

A.H. Nayfeh* and A. Padhye†
Virginia Polytechnic Institute and State University, Blacksburg, Va.

An analysis is presented of the stability of three-dimensional incompressible, isothermal boundary-layer flows. The method of multiple scales is used to derive partial-differential equations that describe the axial and crossflow variations of the disturbance amplitude, phase, and wavenumbers. This equation is used to derive the expressions that relate the temporal and spatial instabilities. These relations are functions of the complex group velocities. Moreover, this equation is used to derive the expression that relates the spatial amplification in any direction to a calculated amplification in any other direction. These relations are verified by numerical results obtained for two- and three-dimensional disturbances in two- and three-dimensional flows.

I. Introduction

IN this article, we consider the relation between the temporal and spatial stabilities for two- as well as three-dimensional incompressible flows. Gaster[1] showed that for a two-dimensional flow, the spatial growth rate is related to the temporal growth rate through the real group velocity. The errors introduced due to the use of the phase velocity in place of the group velocity are negligible only for a nondispersive system of a weakly dispersive system.[2]

In the case of two-dimensional flows and two-dimensional disturbances, it is known in advance that the directions of propagation and amplification are the same, namely, the streamwise direction. On the other hand, for a three-dimensional disturbance, the direction of amplification of a disturbance is not known a priori and must be determined as part of the solution, even for a two-dimensional flow. Because of this difficulty, the direction of amplification is sometimes taken along the phase velocity or the real group velocity.[3]

The purpose of this paper is to establish the relation between three-dimensional temporal and spatial stabilities as well as the relation between spatial stabilities along two directions for two- and three-dimensional flows. We also wish to introduce a new method of calculating the group velocity that is more accurate and less time-consuming than the commonly used finite-difference technique.

Here, we use the method of multiple scales[4] to derive a partial-differential equation that governs the temporal and spatial modulations of the amplitude and the phase of a three-dimensional wave in two- and three-dimensional, incompressible, nonparallel mean flows. This equation can be used to relate the temporal and spatial growth rates as well as the wavenumbers and frequencies. In a quasiparallel flow, it is shown that any spatial growth rate can be transformed into a temporal growth rate, while a temporal growth rate can be transformed into a spatial growth rate along any specified direction. Moreover, a spatial growth rate along a given direction can be related to a spatial growth rate along any other direction.

Presented as Paper 78-1196 at the AIAA 11th Fluid and Plasma Dynamics Conference, Seattle, Wash., July 10-12, 1978; submitted Dec. 26, 1978; revision received April 23, 1979.

Index category: Boundary-Layer Stability and Transition.

*University Distinguished Professor, Engineering Science and Mechanics Dept. Member AIAA.

†Graduate Research Assistant, Engineering Science and Mechanics Dept.

II. Problem Formulation and Asymptotic Solution

We consider the stability of a three-dimensional incompressible, nonparallel boundary layer. We introduce dimensionless quantities using the distance L^* measured from the initiation of the boundary layer and the chordwise velocity U^*, the density ρ^*, and the kinematic viscosity ν^* at the edge of the boundary layer. Solving dimensionless steady boundary-layer equations yields the velocity components

$$U(x_1,z_1,y), \quad \epsilon V(x_1,z_1y), \quad W(x_1,z_1,y) \tag{1}$$

in the x,y, and z directions and the pressure $P(x_1,z_1)$. In these equations,

$$\epsilon=R^{-1}, \qquad R=(U^*L^*/\nu^*)^{1/2}$$

and $x_1=\epsilon x$ and $z_1=\epsilon z$. We superpose the small unsteady disturbances u,v,w and p on this basic flow. The dimensionless linearized equations satisfied by these disturbances are

$$\frac{\partial u}{\partial x}+\frac{\partial v}{\partial y}+\frac{\partial w}{\partial z}=0 \tag{2}$$

$$\frac{\partial u}{\partial t}+U\frac{\partial u}{\partial x}+W\frac{\partial u}{\partial z}+v\frac{\partial U}{\partial y}+\frac{\partial p}{\partial x}-\frac{1}{R}\nabla^2 u = -\epsilon\left[u\frac{\partial U}{\partial x_1}+V\frac{\partial u}{\partial y}+w\frac{\partial U}{\partial z_1}\right]+O(\epsilon^2) \tag{3}$$

$$\frac{\partial v}{\partial t}+U\frac{\partial v}{\partial x}+W\frac{\partial v}{\partial z}+\frac{\partial p}{\partial y}-\frac{1}{R}\nabla^2 v = -\epsilon\left[V\frac{\partial v}{\partial y}+v\frac{\partial V}{\partial y}\right]+O(\epsilon^2) \tag{4}$$

$$\frac{\partial w}{\partial t}+U\frac{\partial w}{\partial x}+W\frac{\partial w}{\partial z}+v\frac{\partial W}{\partial y}+\frac{\partial p}{\partial z}-\frac{1}{R}\nabla^2 w = -\epsilon\left[u\frac{\partial W}{\partial x_1}+V\frac{\partial w}{\partial y_1}+w\frac{\partial W}{\partial z_1}\right]+O(\epsilon^2) \tag{5}$$

We seek a solution to Eqs. (2-5) in the form

$$u=[u_0(x_1,z_1,T_1,y)+\epsilon u_1(x_1,z_1,T_1,y)+\ldots]\exp(i\theta) \tag{6}$$

$$v=[v_0(x_1,z_1,T_1,y)+\epsilon v_1(x_1,z_1,T_1,y)+\ldots]\exp(i\theta) \quad (7)$$

$$w=[w_0(x_1,z_1,T_1,y)+\epsilon w_1(x_1,z_1,T_1,y)+\ldots]\exp(i\theta) \quad (8)$$

$$p=[p_0(x_1,z_1,T_1,y)+\epsilon p_1(x_1,z_1,T_1,y)+\ldots]\exp(i\theta) \quad (9)$$

where $T_1=\epsilon t$ and

$$\frac{\partial\theta}{\partial t}=-\omega, \quad \frac{\partial\theta}{\partial x}=\alpha(x_1,z_1), \quad \frac{\partial\theta}{\partial z}=\beta(x_1,z_1) \quad (10)$$

The solution of the zeroth-order problem can be written as

$$u_0=A(x_1,z_1,T_1)\zeta_1(x_1,z_1;y) \quad (11)$$

$$v_0=A(x_1,z_1,T_1)\zeta_2(x_1,z_1;y) \quad (12)$$

$$w_0=A(x_1,z_1,T_1)\zeta_3(x_1,z_1;y) \quad (13)$$

$$p_0=A(x_1,z_1,T_1)\zeta_4(x_1,z_1;y) \quad (14)$$

where the ζ_n are the eigenmodes of the quasiparallel problem and A is an undetermined complex function.

The equations satisfied by u_1, v_1, w_1, and p_1 are nonhomogenous equations whose homogenous parts have a nontrivial solution. Hence, the nonhomogenous equations have a solution if, and only if, a solvability condition is satisfied. This solvability condition can be written as

$$g_1\frac{\partial A}{\partial T_1}+g_2\frac{\partial A}{\partial x_1}+g_3\frac{\partial A}{\partial z_1}=h_1A \quad (15)$$

where the g_n and h_1 are given in quadratures in terms of the mean-flow quantities, the eigenmodes ζ_n, the eigenmodes of the adjoint problem ζ_n^*, the wavenumber vector $\boldsymbol{k}=\alpha\boldsymbol{e}_x+\beta\boldsymbol{e}_z$, and the x_1 and z_1 derivatives of these quantities (see the Appendix).

To obtain the derivatives of ζ_n with respect to x_1 and z_1, we differentiate the equations satisfied by the ζ_n. These equations are nonhomogenous. Since the homogenous parts of these equations have a nontrivial solution, we need two more solvability conditions which can be written as

$$g_2\frac{\partial\alpha}{\partial x_1}+g_3\frac{\partial\alpha}{\partial z_1}=h_2 \quad (16)$$

$$g_2\frac{\partial\beta}{\partial x_1}+g_3\frac{\partial\beta}{\partial z_1}=h_3 \quad (17)$$

Here, again h_2 and h_3 are given in quadratures in terms of ζ_n, ζ_n^*, α, β, and the x_1 and z_1 derivatives of U and W (see the Appendix).

Equations (15-17) are the main theme of this paper. The h_n in these equations are functions of x_1 and z_1 for a nonparallel flow, but they vanish in the case of a quasiparallel flow. Next, we use these equations to relate the temporal and spatial instabilities for the case of quasiparallel flow.

The complex group velocities ω_α and ω_β in the x and z directions are related to the g_n by

$$\frac{g_2}{g_1}=\frac{\partial\omega}{\partial\alpha}=\omega_\alpha \text{ and } \frac{g_3}{g_1}=\frac{\partial\omega}{\partial\beta}=\omega_\beta \quad (18a)$$

The commonly used method for calculating the group velocity is based on finite differences and using the approximation

$$\frac{\partial\omega}{\partial\alpha}=\frac{\Delta\omega}{\Delta\alpha} \text{ and } \frac{\partial\omega}{\partial\beta}=\frac{\Delta\omega}{\Delta\beta} \quad (18b)$$

With Eq. (18a) and the Appendix, we merely need to solve an adjoint problem and evaluate the g_n in quadratures. This gives an easier and shorter way of calculating the group velocity which does not sacrifice accuracy.

For a quasiparallel mean flow, $h_n=0$ for $n=1$, 2, and 3; and to the first approximation

$$u=A(x,z,t)\zeta_1(y)\exp[i(\alpha x+\beta z-\omega t)] \quad (19)$$

$$v=A(x,z,t)\zeta_2(y)\exp[i(\alpha x+\beta z-\omega t)] \quad (20)$$

$$w=A(x,z,t)\zeta_3(y)\exp[i(\alpha x+\beta z-\omega t)] \quad (21)$$

$$p=A(x,z,t)\zeta_4(y)\exp[i(\alpha x+\beta z-\omega t)] \quad (22)$$

where

$$\frac{\partial A}{\partial t}+\omega_\alpha\frac{\partial A}{\partial x}+\omega_\beta\frac{\partial A}{\partial z}=0 \quad (23)$$

$$\omega_\alpha\frac{\partial\alpha}{\partial x}+\omega_\beta\frac{\partial\alpha}{\partial z}=0 \quad (24)$$

$$\omega_\alpha\frac{\partial\beta}{\partial x}+\omega_\beta\frac{\partial\beta}{\partial z}=0 \quad (25)$$

A. Spatial Stability

For a spatial stability, ω is real and fixed, while α and β are complex. If we write

$$a=A\exp[-(\alpha_i x+\beta_i z)] \quad (26)$$

where α_i and β_i are the imaginary parts of α and β, respectively, then we may rewrite Eq. (19) as

$$u=a(x,z,t)\zeta_1(y)\exp[i(\alpha_r x+\beta_r z-\omega t)] \quad (27)$$

where α_r and β_r are the real parts of α and β. Equations (20-22) also can be written in a form similar to Eq. (27). It follows from Eq. (26) that

$$A=a\exp(\alpha_i x+\beta_i z) \quad (28)$$

Hence, Eq. (23) becomes

$$\frac{\partial a}{\partial t}+\omega_\alpha\frac{\partial a}{\partial x}+\omega_\beta\frac{\partial a}{\partial z}=-(\omega_\alpha\alpha_i+\omega_\beta\beta_i)a \quad (29)$$

B. Temporal Stability

In the case of a temporal stability, α and β are real and fixed, while $\omega=\omega_r+i\omega_i$. Then we may write

$$u=a(x,z,t)\zeta_1(y)\exp[i(\alpha x+\beta z-\omega_r t)] \quad (30)$$

where

$$a=A\exp(\omega_i t) \text{ or } A=a\exp(-\omega_i t) \quad (31)$$

Using Eq. (31) in Eq. (23), we obtain

$$\frac{\partial a}{\partial t}+\omega_\alpha\frac{\partial a}{\partial x}+\omega_\beta\frac{\partial a}{\partial z}=\omega_i a \quad (32)$$

III. Two-Dimensional Stability

In this case, a is a function of x and t only and $\beta\equiv 0$. Hence, Eqs. (29) and (32) become

$$\frac{\partial a}{\partial t}+\omega_\alpha\frac{\partial a}{\partial x}=-\omega_\alpha\alpha_i a \quad (33)$$

$$\frac{\partial a}{\partial t}+\omega_\alpha\frac{\partial a}{\partial x}=\omega_i a \tag{34}$$

A. Converting from a Spatial to a Temporal Stability

In this case, we constrain a to be independent of x in Eq. (33). The solution of the resulting equation is

$$a=a_0\exp(-\omega_\alpha\alpha_i t) \tag{35}$$

where a_0 is a constant. Expressing ω_α in the polar form $c_g\exp(i\chi)$, we rewrite Eq. (35) as

$$a=a_0\exp[-(\alpha_i c_g\cos\chi+i\alpha_i c_g\sin\chi)t] \tag{36}$$

Hence, Eq. (27) becomes

$$u=a_0\zeta_1(y)\exp\{i[\alpha_r x-(\omega+\delta\omega)t]+\sigma_t t\} \tag{37}$$

where

$$\sigma_t=-\alpha_i c_g\cos\chi,\quad \delta\omega=\alpha_i c_g\sin\chi \tag{38}$$

Thus, the spatial stability has been transformed into a temporal stability with the growth rate σ_t and a corresponding shift $\delta\omega$ in the frequency.

B. Converting from a Temporal to a Spatial Stability

In this case, we constrain a to be independent of t in Eq. (34), solve the resulting equation, and obtain

$$a=a_0\exp(\omega_i x/\omega_\alpha) \tag{39}$$

Expressing ω_α in polar form and substituting into Eq. (30), we have

$$u=a_0\zeta_1(y)\exp\{i[(\alpha+\delta\alpha)x-\omega_r t]+\sigma_s x\} \tag{40}$$

where

$$\sigma_s=\frac{\omega_i}{c_g}\cos\chi,\quad \delta\alpha=-\frac{\omega_i}{c_g}\sin\chi \tag{41}$$

Thus, the temporal stability is transformed into a spatial stability with the growth rate σ_s, with a corresponding shift $\delta\alpha$ in the wavenumber.

To verify the validity of the proposed transformation, we calculated the two-dimensional temporal and spatial stabilities of the Blasius flow for an $F=\omega/R=110\times10^{-6}$ and different Reynolds numbers. The results are shown in Tables 1 and 2. In Table 1, for each R and ω, a complex α is determined from the eigenvalue problem and listed in column 2. The complex group velocity expressed in polar form and determined from the spatial stability is listed in columns 3 and 4. Using these values, we calculated the phase shift $\delta\omega$ and the transformed temporal growth rate σ_t from Eqs. (38); they are listed in columns 6 and 7. In Table 2, for each R and α, a complex ω is determined and listed in column 2. The complex group velocity expressed in polar form and calculated from the temporal stability is listed in columns 3 and 4. Using these values, we calculated the wavenumber shift $\delta\alpha$ and transformed spatial growth rate σ_s from Eqs. (41); they are listed in columns 6 and 7. Comparing the group velocities in Tables 1 and 2, we observe that they are in close agreement, and hence the group velocity can be calculated fairly accurately by using either the temporal or spatial stability. Moreover, comparing the temporal growth rate ω_i in Table 2, which was calculated from the temporal stability, with the temporal growth rate σ_t in Table 1, which was calculated by using the proposed transformation, we find that they are in very good agreement. Furthermore, comparing the spatial growth rate α_i in Table 1, which was calculated from the spatial stability, with the spatial growth rate σ_s in Table 2, which was calculated by using the proposed transformation, we find again that they are in very good agreement.

IV. Three-Dimensional Stability

In this case, the governing equations are Eqs. (29) and (32).

A. Converting from a Spatial to a Temporal Stability

To convert a spatial stability into a temporal stability, we constrain a to be independent of x and z in Eq. (29) and obtain

$$\frac{da}{dt}=-(\omega_\alpha\alpha_i+\omega_\beta\beta_i)a \tag{42}$$

Table 1 Transformation of a two-dimensional spatial instability to a temporal instability for the Blasius flow for $F=110\times10^{-6}$; $\omega_\alpha=c_g\exp(i\chi)$

R	$\alpha=\alpha_r+i\alpha_i$	Group velocity c_g	Group velocity χ, deg	Frequency, ω	Frequency shift, $\delta\omega$	Transformed temporal growth rate, σ_t
400	(0.1238, 0.1917E-3)	0.4355	5.927	0.04400	0.8621E-5	−0.8304E-4
450	(0.1380, −0.2072E-2)	0.4313	3.862	0.04950	−0.6019E-4	0.8917E-3
475	(0.1452, −0.2896E-2)	0.4293	2.603	0.05225	−0.5647E-4	0.1242E-2
500	(0.1525, −0.3487E-2)	0.4275	1.208	0.05500	−0.3144E-4	0.1490E-2
550	(0.1672, −0.3888E-2)	0.4247	− 1.975	0.06050	0.5692E-4	0.1650E-2
600	(0.1819, −0.3113E-2)	0.4236	− 5.715	0.06600	0.1313E-3	0.1312E-2
640	(0.1937, −0.1532E-2)	0.4244	− 9.177	0.07040	0.1037E-3	0.6418E-3
670	(0.2023, 0.2727E-3)	0.4266	−12.112	0.07370	−0.2441E-4	0.1137E-3

Table 2 Transformation of a two-dimensional temporal instability to a spatial instability for the Blasius flow for $F\approx100\times10^{-6}$; $\omega_\alpha=c_g\exp(i\chi)$

R	$\omega=\omega_r+i\omega_i$	Group velocity c_g	Group velocity χ, deg	α	Wavenumber shift, $\delta\alpha$	Transformed spatial growth rate, σ_s
400	(0.0440, −0.8302E-4)	0.4353	5.916	0.1238	0.1966E-4	−0.1897E-3
450	(0.0494, 0.8939E-3)	0.4335	3.958	0.1380	−0.1424E-3	0.2057E-2
475	(0.0522, 0.1247E-2)	0.4326	2.725	0.1452	−0.1370E-3	0.2879E-2
500	(0.0550, 0.1498E-2)	0.4318	1.341	0.1525	−0.8121E-4	0.3469E-2
550	(0.0606, 0.1662E-2)	0.4303	− 1.857	0.1672	0.1251E-3	0.3860E-2
600	(0.0661, 0.1320E-2)	0.4287	− 5.643	0.1819	0.3028E-3	0.3064E-2
640	(0.0705, 0.6444E-3)	0.4273	− 9.150	0.1937	0.2398E-3	0.1489E-2
670	(0.0737, −0.1137E-3)	0.4260	−12.115	0.2023	−0.5601E-4	−0.2609E-3

which has the solution

$$a=a_0\exp[-(\omega_\alpha\alpha_i+\omega_\beta\beta_i)t] \tag{43}$$

where a_0 is a constant. It is convenient to define a spatial growth rate σ_s and a growth rate direction $\bar{\psi}$ according to

$$\alpha_i=-\sigma_s\cos\bar{\psi},\quad \beta_i=-\sigma_s\sin\bar{\psi} \tag{44}$$

Moreover, it is convenient to express the complex group-velocity components in the form

$$\omega_\alpha=\cos\phi,\quad \omega_\beta=c\sin\phi \tag{45}$$

where c and ϕ are complex. Then Eq. (43) can be rewritten as

$$a=a_0\exp[\sigma_s c\cos(\phi-\bar{\psi})t] \tag{46}$$

Substituting for a from Eq. (46) into Eq. (27), we have

$$u=a_0\zeta_1(y)\exp\{i[\alpha_r x+\beta_r z-(\omega+\delta\omega)t]+\sigma_t t\} \tag{47}$$

where

$$\sigma_t-i\delta\omega=\sigma_s c\cos(\phi-\bar{\psi}) \tag{48}$$

Hence, a spatial-stability problem can be converted into a temporal-stability problem having the growth rate σ_t and a frequency shifted from ω by $\delta\omega$, where σ_t and $\delta\omega$ are defined by Eq. (48).

B. Converting from a Temporal to a Spatial Stability along a Given Direction

Converting from a temporal to a spatial stability is more involved. In this case, we restrict a to be independent of t in Eq. (32) and obtain

$$\omega_\alpha\frac{\partial a}{\partial x}+\omega_\beta\frac{\partial a}{\partial z}=\omega_i a \tag{49}$$

We note that $\omega_\beta/\omega_\alpha$ is complex in general, and hence Eq. (49) is elliptic. Since for a physical problem, the equation describing a must be hyperbolic, Nayfeh[5] concluded that the values of α and β must be such that $g_3/g_2=\omega_\beta/\omega_\alpha$ is real. For a parallel mean flow, this condition reduces to $\partial\alpha/\partial\beta$ must be real, which was derived by Cebeci and Stewartson[6] and Nayfeh[5] using the saddle-point method.

One might argue that if the imaginary parts of ω_α and ω_β are small compared with the real parts, then the imaginary terms belong to the second-order problem rather than the first. Certainly, this is the case if the imaginary parts of ω_α and ω_β are small compared with $\omega_{\alpha\alpha}$, $\omega_{\alpha\beta}$, and $\omega_{\beta\beta}$. However, for the weakly dispersive problem with which we are dealing, this is not always the case. In his analysis of wavepackets by using the saddle-point method, Gaster[7] found out that neglecting these imaginary parts predicts wavepackets which contain wave caustics toward their outer regions. A more careful examination of the magnitudes of the imaginary parts of ω_α and ω_β with respect to $\omega_{\alpha\alpha}$ and $\omega_{\beta\beta}$ shows that they are of the same order. Keeping the imaginary parts and using a saddle-point expansion, he found that the wave caustics disappear.[8]

For propagation along any direction ξ inclined at an angle $\bar{\psi}$ from the x direction, we let

$$\xi=x\cos\bar{\psi}+z\sin\bar{\psi} \tag{50}$$

and

$$\eta=-x\sin\bar{\psi}+z\cos\bar{\psi} \tag{51}$$

where η is normal to ξ. Substituting Eqs. (50) and (51) into Eq. (49) gives

$$(\omega_\alpha\cos\bar{\psi}+\omega_\beta\sin\bar{\psi})\frac{\partial a}{\partial\xi}+(\omega_\beta\cos\bar{\psi}-\omega_\alpha\sin\bar{\psi})\frac{\partial a}{\partial\eta}=\omega_i a \tag{52}$$

Now, if we restrict a to be independent of η and use Eq. (45), we obtain

$$\frac{\partial a}{\partial\xi}=\frac{\omega_i a}{c\cos(\phi-\bar{\psi})} \tag{53}$$

which has the solution

$$a=a_0\exp\left[\frac{\omega_i}{c\cos(\phi-\bar{\psi})}\xi\right] \tag{54}$$

Substituting Eq. (54) into Eq. (30) yields

$$u=a_0\zeta_1(\eta)\exp\{\sigma_x x+\sigma_z z+i[(\alpha+\delta\alpha)x+(\beta+\delta\beta)z-\omega t]\} \tag{55}$$

where

$$\delta\alpha-i\sigma_x=-i\frac{\omega_i\cos\bar{\psi}}{c\cos(\phi-\bar{\psi})} \tag{56}$$

and

$$\delta\beta-i\sigma_z=-i\frac{\omega_i\sin\bar{\psi}}{c\cos(\phi-\bar{\psi})} \tag{57}$$

From these equations, we can obtain the growth rates σ_x and σ_z in the x and z directions as well as the shifts $\delta\alpha$ and $\delta\beta$ in the components of the wavenumber.

For example, to convert from a temporal stability to a spatial stability along the x direction, we select $\bar{\psi}$ to be zero. Then,

$$\delta\alpha-i\sigma_x=-\frac{i\omega_i}{c\cos\phi} \tag{58}$$

and

$$\delta\beta=0 \tag{59}$$

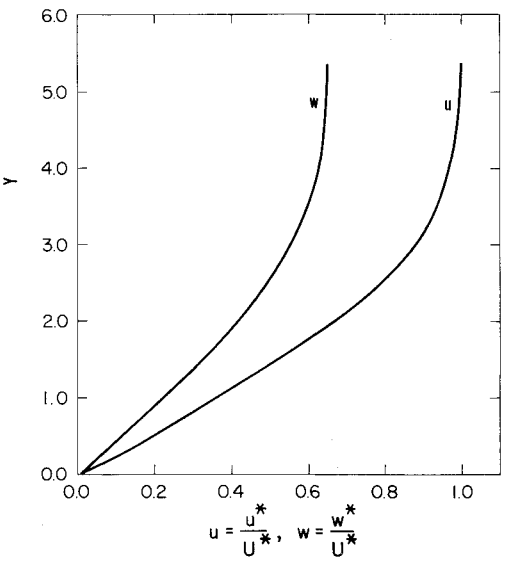

Fig. 1 Three-dimensional boundary-layer profile for sweptback wing. L.E. sweep: 33 deg; T.E. sweep: 19 deg; $U_\infty=290.43$ fps; chord $\hat{c}=14.66$; $x/\hat{c}=0.175$; $R=1153.7$.

Table 3 Transformation of temporal growth rate into spatial growth rate along a direction given by $\overline{\psi}$ for a three-dimensional boundary-layer flow at $R = 1153.7$

α_r	$\beta_r \times 10^2$	$\omega = \omega_r + i\omega_i$	ω_α	ω_β	$\overline{\psi}_0$	σ_x Eq. (56)	σ_z Eq. (57)
0.07	4.0415	(2.6180E-2, 3.5579E-4)	(0.3349, 5.6539E-2)	(0.2109, 4.1424E-2)	30.0	7.5557E-4	4.3623E-4
0.07	4.0415	(2.6180E-2, 3.5579E-4)	(0.3349, 5.6539E-2)	(0.2109, 4.1424E-2)	50.0	5.8764E-4	7.0033E-4
0.07	5.8737	(3.0261E-2, 1.1205E-3)	(0.3307, 4.6722E-2)	(0.2336, 4.0473E-2)	30.0	2.3535E-3	1.3588E-3
0.07	8.3423	(3.6321E-2, 1.9911E-3)	(0.3264, 3.0663E-2)	(0.2558, 2.7918E-2)	30.0	4.1594E-3	2.4014E-3
0.07	8.3423	(3.6321E-2, 1.9911E-3)	(0.3264, 3.0663E-2)	(0.2558, 2.7918E-2)	40.0	3.6437E-3	3.0574E-3
0.07	12.124	(4.6422E-2, 2.4267E-3)	(0.3236, 3.4352E-3)	(0.2756, −7.923E-3)	30.0	5.0272E-3	2.9024E-3

Table 4 Transformation of spatial growth rate into temporal growth rate for a three-dimensional boundary layer flow at $R = 1153.7$

$\alpha = \alpha_r + i\alpha_i$	$\beta = \beta_r + i\beta_i$	ω_r	ω_α	ω_β	σ_t Eq. (48)
(6.9867E-2, −7.5609E-4)	(4.0338E-2, −4.3653E-4)	2.6180E-2	(0.3344, 5.5951E-2)	(0.2106, 4.1039E-2)	3.4479E-4
(6.9894E-2, −5.8810E-4)	(4.0288E-2, −7.0087E-4)	2.6180E-2	(0.3344, 5.6191E-2)	(0.2107, 4.0621E-2)	3.4569E-4
(7.0033E-2, −2.3524E-3)	(5.7990E-2, −1.3582E-3)	3.0261E-2	(0.3293, 3.9733E-2)	(0.2310, 3.9733E-2)	1.0883E-3
(6.9597E-2, −4.1906E-3)	(8.3195E-2, −2.4194E-3)	3.6321E-2	(0.3224, 2.6982E-2)	(0.2512, 2.7221E-2)	1.9587E-3
(6.9641E-2, −3.6725E-3)	(8.3124E-2, −3.0816E-3)	3.6321E-2	(0.3222, 2.7629E-2)	(0.2510, 2.6703E-2)	1.9569E-3
(7.0024E-2, −5.0782E-3)	(1.2127E-1, −2.9319E-3)	4.6422E-2	(0.3177, 3.9813E-3)	(0.2685, −8.540E-3)	2.4004E-3

Table 5 Transformation of a spatial growth rate along the direction $\overline{\psi}_1$ into a spatial growth rate along the direction $\overline{\psi}_2$ [a]

	From transformation			From eigenvalue problem	
$\overline{\psi}$, deg	ψ_2, deg	$k_2 \times 10$	$\sigma_{s_2} \times 10^3$	$k_2 \times 10$	$\sigma_{s_2} \times 10^3$
20.0	49.986	1.6688	3.1902	1.6688	3.1906
40.0	49.988	1.6701	3.6408	1.6701	3.6428
60.0	50.029	1.6729	4.9166	1.6729	4.9257
80.0	50.332	1.6851	9.1230	1.6852	9.2056

[a] Blasius profile, $R = 1600$, $F = 2.225 \times 10^{-5}$, $\psi_1 = 50$ deg, $\overline{\psi}_1 = 0.0$ deg, $\sigma_{s_1} = 3.1760 \times 10^{-3}$, $k_1 = 0.16682$, $\tan\phi = (0.16149, -0.07222)$.

Table 6 Transformation of a spatial growth rate along the direction $\overline{\psi}_1$ into a spatial growth rate along the direction $\overline{\psi}_2$ [a]

	From transformation			From eigenvalue problem	
$\overline{\psi}_2$, deg	ψ_2, deg	$k_2 \times 10^2$	$\sigma_{s_2} \times 10^3$	$k_2 \times 10^2$	$\sigma_{s_1} \times 10^3$
0.0	20.003	9.0913	4.6619	9.0931	4.6612
20.0	20.0	9.0917	4.7898	9.0923	4.7896
60.0	20.008	9.0938	7.9677	9.0953	7.9651
80.0	20.090	9.1007	17.2378	9.1236	17.0827

[a] Blasius profile, $R = 1600$, $F = 1.49 \times 10^{-5}$, $\psi_1 = 20$ deg, $\overline{\psi}_1 = 40$ deg, $\sigma_{s1} = 5.6222 \times 10^{-3}$, $k_1 = 9.0924 \times 10^{-2}$, $\tan\phi = (0.98261 \times 10^{-1}, -0.33341 \times 10^{-2})$.

On the other hand, to convert from a temporal stability to a spatial stability along the z direction, we select $\overline{\psi}$ to be 90 deg. Then

$$\delta\alpha = 0 \tag{60}$$

and

$$\delta\beta - i\sigma_z = -i\frac{\omega_i}{c\sin\phi} \tag{61}$$

To validate Eqs. (48), (56), and (57), we performed calculations for the velocity profile shown in Fig. 1 computed for a sweptback wing at $R = 1153.7$. For the fixed real values of α and β listed in columns 1 and 2 of Table 3, we calculated the complex eigenvalue ω, listed in column 3. The corresponding complex group-velocity components are listed in columns 4 and 5. Then using Eqs. (56) and (57) and the growth rate directions listed in column 6, we calculated the components σ_x and σ_z of the spatial growth rate σ_s; these are listed in columns 7 and 8. Also, the shifts $\delta\alpha$ and $\delta\beta$ in the components of wavenumber were calculated. For the values of ω_r and $\overline{\psi}$ in Table 3 and the corresponding wave angle $\psi = \tan^{-1}[(\beta_r - \delta\beta)/(\alpha_r - \delta\alpha)]$, we computed the complex values α and β from the eigenvalue problem. These are listed in columns 1 and 2 of Table 4. Comparing α_i and β_i from Table 4 with σ_x and σ_z from Table 3, we conclude that the proposed transformation is fairly accurate. Using the complex-group velocity components and the values of α and β in Table 4, we used Eq. (48) to convert the spatial stability to a temporal stability with the growth rate σ_t listed in column 6 of Table 4. Comparing this value with ω_i in column 3 of Table 3, we conclude that the proposed transformation is again fairly accurate.

C. Converting from a Spatial Stability to a Spatial Stability along a Different Direction

In this case, we restrict a to be independent of t in Eq. (29), and obtain

$$\omega_\alpha \frac{\partial a}{\partial x} + \omega_\beta \frac{\partial a}{\partial z} = -(\alpha_i\omega_\alpha + \beta_i\omega_\beta)a \tag{62}$$

If the growth direction is $\overline{\psi}$ and the spatial growth rate is σ_{s1}, Eq. (62) can be rewritten as

$$\omega_\alpha \frac{\partial a}{\partial x} + \omega_\beta \frac{\partial a}{\partial z} = \sigma_{s1} c a \cos(\phi - \overline{\psi}_1) \tag{63}$$

Table 7a Transformation of a spatial growth rate along the direction $\bar{\psi}_1$ into a spatial growth ate along the direction $\bar{\psi}_2$ [a]

	From transformation			From eigenvalue problem	
$\bar{\psi}_2$, deg	ψ_2, deg	$k_2 \times 10$	$\sigma_{s_2} \times 10^3$	$k_2 \times 10$	$\sigma_{s_2} \times 10^3$
0.0	30.011	1.7754	2.5051	1.7754	2.5059
20.0	30.002	1.7756	2.5522	1.7756	2.5524
60.0	30.015	1.7768	4.1264	1.7768	4.1272
80.0	30.184	1.7808	8.4167	1.7810	8.4306

[a] Balsius profile, $R=525$, $F=1.1\times10^{-3}$, $\psi_1=30$ deg, $\bar{\psi}_1=40$ deg, $\sigma_{s_1}=2.9645\times10^{-3}$, $k_1=0.17760$, $\tan\phi=(0.12285, -0.34383+10^{-1})$.

Table 7b Transformation of a spatial growth rate along the direction $\bar{\psi}_1$ into a spatial growth rate along the direction $\bar{\psi}_2$ [a]

	From transformation			From eigenvalue problem	
$\bar{\psi}_1$, deg	ψ_2, deg	$k_2 \times 10$	$\sigma_{s_2} \times 10^3$	$k_2 \times 10$	$\sigma_{s_2} \times 10^3$
0.0	30.054	1.7757	2.4880	1.7759	2.5011
20.0	29.983	1.7755	2.5407	1.7758	2.5507
40.0	29.983	1.7755	2.9591	1.7707	2.9669
60.0	29.949	1.7759	4.1354	1.7759	4.1403

[a] Blasius profile, $R=525$, $F=1.1\times10^{-4}$, $\psi_1=30$ deg, $\bar{\psi}_1=80$ deg, $\sigma_{s_1}=8.5142\times10^{-3}$, $k_1=0.17786$, $\tan\phi=(0.12039, -0.39832+10^{-1})$.

Table 8 Transformation of a spatial growth rate along the direction $\bar{\psi}_1$ into a spatial growth rate along the direction $\bar{\psi}_2$ [a]

	From transformation			From eigenvalue problem	
$\bar{\psi}_2$, deg	ψ_2, deg	$k_2 \times 10^2$	$\sigma_{s_2} \times 10^3$	$k_2 \times 10^2$	$\sigma_{s_2} \times 10^3$
20.0	40.005	8.7508	2.2606	8.7509	2.2603
40.0	40.000	8.7490	2.1877	9.7495	2.1872
60.0	39.986	8.7470	2.3995	8.7483	2.3988
80.0	39.952	8.7440	3.0654	8.7469	3.0639

[a] Three-dimensional velocity profile, $R=1153.7$, $F=2.4998\times10^{-5}$, $\psi_1=40$ deg, $\bar{\psi}_1=0.0$ deg, $\sigma_{s_1}=2.6714\times10^{-3}$, $k_1=0.08753$, $\tan\phi=(0.70733, 0.03316)$.

on account of Eqs. (44) and (45). To transform the growth rate from σ_{s_1} in the $\bar{\psi}_1$ direction to σ_{s_2} in the $\bar{\psi}_2$ direction, we use Eqs. (50) and (51) with $\bar{\psi}$ replaced with $\bar{\psi}_2$, use Eq. (45), and rewrite Eq. (63) as

$$c\cos(\phi-\bar{\psi}_2)\frac{\partial a}{\partial \xi}+c\sin(\phi-\bar{\psi}_2)\frac{\partial a}{\partial \eta}=\sigma_{s_1}ca\cos(\phi-\bar{\psi}_1) \quad (64)$$

If we restrict a to be independent of η and solve the resulting equation, we obtain

$$a=a_0\exp[\xi\sigma_{s_1}\cos(\phi-\bar{\psi}_1)/\cos(\phi-\bar{\psi}_2)] \quad (65)$$

Hence, the growth rate σ_{s_2} in the $\bar{\psi}_2$ direction is given by

$$\sigma_{s_2}=\sigma_{s_1}Re[\cos(\phi-\bar{\psi}_1)/\cos(\phi-\bar{\psi}_2)] \quad (66)$$

while the shifts $\delta\alpha_r$ and $\delta\beta_r$ in the components of the wavenumber are given by

$$(\delta\alpha_r,\delta\beta_r)$$

$$=\sigma_{s_1}(\cos\bar{\psi}_2,\sin\bar{\psi})\mathrm{Im}[\cos(\phi-\bar{\psi}_1)/\cos(\phi-\bar{\psi}_2)] \quad (67)$$

To validate Eq. (66), we performed calculations for the Blasius flow as well as for a flow over a sweptback wing. For the Blasius flow at a Reynolds number $R=1600$ and a frequency $F=2.225\times10^{-5}$, we calculated the spatial growth rate σ_{s_1}, the wavenumber k_1, and the complex group-velocity ratio $\tan\phi$ for a disturbance having the wave angle $\psi_1=50$ deg and the growth direction $\bar{\psi}_1=0$. Using these values and Eqs. (66) and (67), we predicted σ_{s_2}, k_2, and ψ_2 for several values of $\bar{\psi}_2$; four such calculations are listed in Table 5. Using the values of ψ_2 and $\bar{\psi}_2$ listed in columns 1 and 2, we determined σ_{s_2} and k_2 from the eigenvalue problem and listed them in columns 5 and 6 of Table 5. Comparing columns 3 and 4 with columns 5 and 6 shows that k_2 is predicted to within four significant figures, while the maximum error in the prediction of σ_{s_2} is about 0.9%.

For the Blasius flow at $R=1600$ and $F=2.225\times10^{-5}$, we calculated σ_{s_1}, k_1, $\tan\phi_1$ for a disturbance with $\psi_1=20$ deg and $\bar{\psi}_1=40$ deg. Using these values and Eqs. (66) and (67), we predicted σ_{s_2}, k_2, and ψ_2; for several values of $\bar{\psi}_2$, four such calculations are listed in Table 6. Using the values of ψ_2 and $\bar{\psi}_2$ listed in columns 1 and 2 of this table, we calculated σ_{s_2} and k_2 from the eigenvalue problem and listed them in columns 5 and 6 of Table 6. Comparing columns 3 and 4 with columns 5 and 6 shows that the maximum error in the predicted value of k_2 is about 0.3%, while the maximum error in the predicted value of σ_{s_2} is about 0.9%.

Similar calculations were performed for the Blasius flow at $R=525$ and $F=1.1\times10^{-4}$. In Table 7a, the spatial growth rate for $\psi_1=30$ deg and $\bar{\psi}_1=40$ deg is transformed into spatial growth rates along four other directions. In Table 7b, the spatial growth rate for $\psi_1=30$ deg and $\bar{\psi}_1=80$ deg is transformed into spatial growth rates along four other directions. These tables show that the maximum error in the predicted k_2 is about 0.01% and the maximum error in the predicted σ_{s_2} is about 0.2%.

To show that the proposed transformation is not limited by the mean flow, we tested it for a flow on a sweptback wing having a leading-edge sweepback angle of 30 deg and a trailing-edge sweepback angle of 19 deg, as shown in Fig. 1. The calculations were performed at the 17.5% chord location at $R=1153.7$ and $F=2.4998\times10^{-5}$. The spatial growth rate for a disturbance with $\psi_1=40$ deg and $\bar{\psi}_1=0$ deg is transformed into spatial growth rates along four other directions. These growth rates, which are listed in column 4 of Table 8,

are in close agreement with those calculated from the eigenvalue problem listed in column 6 of Table 8. The maximum error in the predicted growth rate is about 0.05%.

V. Concluding Remarks

The method of multiple scales has been used to derive partial-differential equations governing the temporal and spatial modulations of the amplitude and the wavenumber of a disturbance in a three-dimensional, incompressible, nonparallel boundary-layer flow. These equations have been used to relate the temporal and spatial growth rates as well as the growth rates along two different directions. The present transformations have been verified for the Blasius flow as well as for three-dimensional incompressible flows past sweptback wings. Using our Eq. (23), Mack[9] proposed a transformation relating the spatial growth rate along one direction to the spatial growth rate along another direction. Recently, calculations by El-Hady and Nayfeh[10] verified these transformations for subsonic and supersonic flows.

Appendix

$$g_1=\int_0^\infty(\zeta_1\zeta_1^*+\zeta_2\zeta_2^*+\zeta_3\zeta_3^*)\,dy$$

$$g_2=\int_0^\infty\left[(\zeta_1\zeta_4^*+\zeta_1^*\zeta_4)+\left(U-\frac{2i\alpha}{R}\right)(\zeta_1\zeta_1^*+\zeta_2\zeta_2^*+\zeta_3\zeta_3^*)\right]dy$$

$$g_3=\int_0^\infty\left[(\zeta_3\zeta_4^*+\zeta_3^*\zeta_4)+\left(W-\frac{2i\beta}{R}\right)(\zeta_1\zeta_1^*+\zeta_2\zeta_2^*+\zeta_3\zeta_3^*)\right]dy$$

$$h_1=\frac{i}{R}\left(\frac{\partial\alpha}{\partial x_1}+\frac{\partial\beta}{\partial x_1}\right)\int_0^\infty(\zeta_1\zeta_1^*+\zeta_2\zeta_2^*+\zeta_3\zeta_3^*)\,dy$$
$$-\int_0^\infty\left[\left(U-\frac{2i\alpha}{R}\right)\left(\frac{\partial\zeta_1}{\partial x_1}\zeta_1^*+\frac{\partial\zeta_2}{\partial x_1}\zeta_2^*+\frac{\partial\zeta_3}{\partial x_1}\zeta_3^*\right)\right.$$
$$+\left(W-\frac{2i\beta}{R}\right)\left(\frac{\partial\zeta_1}{\partial z_1}\zeta_1^*+\frac{\partial\zeta_2}{\partial z_1}\zeta_2^*+\frac{\partial\zeta_3}{\partial z_1}\zeta_3^*\right)$$
$$+\left(\frac{\partial U}{\partial x_1}\zeta_1+\frac{\partial U}{\partial z_1}\zeta_3\right)\zeta_1^*+\left(\frac{\partial W}{\partial x_1}\zeta_1+\frac{\partial W}{\partial z_1}\zeta_3\right)\zeta_3^*$$
$$\left.+\zeta_4^*\left(\frac{\partial\zeta_1}{\partial x_1}+\frac{\partial\zeta_3}{\partial z_1}\right)+\zeta_1^*\frac{\partial\zeta_4}{\partial x_1}+\zeta_1^*\frac{\partial\zeta_4}{\partial z_1}\right]dy$$

and

$$h_2=\int_0^\infty-\left(\alpha\frac{\partial U}{\partial x_1}+\beta\frac{\partial W}{\partial x_1}\right)(\zeta_1\zeta_1^*+\zeta_2\zeta_2^*+\zeta_3\zeta_3^*)$$
$$+i\zeta_2\left[\frac{\partial^2U}{\partial y\partial x_1}\zeta_1^*+\frac{\partial^2W}{\partial y\partial x_1}\zeta_3^*\right]dy$$

$$h_3=\int_0^\infty-\left(\alpha\frac{\partial U}{\partial z_1}+\beta\frac{\partial W}{\partial z_1}\right)(\zeta_1\zeta_1^*+\zeta_2\zeta_2^*+\zeta_3\zeta_3^*)$$
$$+i\zeta_2\left[\frac{\partial^2U}{\partial y\partial z_1}\zeta_1^*+\frac{\partial^2W}{\partial y\partial z_1}\zeta_3^*\right]dy$$

where R = Reynolds number.

Adjoint Problem

$$i\alpha\zeta_1^*+i\beta\zeta_3^*-D\zeta_2^*=0$$

$$i(\alpha U+\beta W-\omega)\zeta_1^*+i\alpha\zeta_4^*-(1/R)[D^2-(\alpha^2\beta^2)]\zeta_1^*=0$$

$$i(\alpha U+\beta W-\omega)\zeta_2^*-D\zeta_4^*+DU\zeta_1^*+DW\zeta_3^*$$
$$-(1/R)[D^2-(\alpha^2+\beta^2)]\zeta_2^*=0$$

$$i(\alpha U+\beta W-\omega)\alpha_3^*+i\beta\zeta_4^*-(1/R)[D^2-(\alpha^2+\beta^2)]\zeta_3^*=0$$

Acknowledgment

This work was supported by the NASA Langley Reseach Center under Grant No. NSG 1255. The comments and discussions of W.S. Saric are greatly appreciated.

References

[1] Gaster, M., "A Note on the Relation between Temporally Increasing and Spatially Increasing Disturbances in Hydrodynamic Stability," *Journal of Fluid Mechanics,* Vol. 14, 1962, pp. 222-224.

[2] Gaster, M., "The Role of Spatially Growing Waves in the Theory of Hydrodynamic Stability," *Progress in Aerospace Sciences,* Vol. 6, 1965, pp. 251-270.

[3] Mack, L.M., "Transition Prediction and Linear-Stability Theory," *AGARD Fluid Dynamics Panel Symposium of Laminar-Turbulent Transition,* Copenhagen, Denmark, May 2-4, 1977.

[4] Nayfeh, A.H., *Perturbation Methods,* Wiley, New York, 1973, Chap. 6.

[5] Nayfeh, A.H., "Stability of Three-Dimensional Boundary Layers," AIAA Paper 79-0262, New Orleans, La., Jan. 1979.

[6] Cebeci, T. and Stewartson, K., "On Stability and Transition in Three-Dimensional Flows," AIAA Paper, 79-0263, New Orleans, La., Jan. 1979.

[7] Gaster, M., "The Development of Three-Dimensional Wave Packets in a Boundary Layer," *Journal of Mechanics,* Vol. 32, 1968, pp. 173-184.

[8] Gaster, M., "On the Application of Ray Mathematics to Non-conservative Systems," *Proceedings National Science Foundation Regional Conference on Geophysical Fluid Dynamical Wave Mathematics,* University of Washington, Seattle, Wa., 1977, pp. 61-66.

[9] Mack, L.M., "Three-Dimensional Effects in Boundary-Layer Stability," *Twelfth Symposium on Naval Hydrodynamics,* Washington, D.C., June 5-9, 1978.

[10] El-Hady, N.M. and Nayfeh, A.H., "Nonparallel Stability of Compressible Boundary-layer Flows," Virginia Polytechnic Institute and State University Rept. No. VPI-E-79-13, 1979.